Observations and simulations of some divergent-light halos

Lars Gislén and Jan O. Mattsson

We deal with some halos generated by the divergent light from a nearby source. After discussing how the divergent light transforms some halo features, we give an outline of a method of handling the simulation of a divergent-light halo. The simulation method is then successfully tested on some well-documented halo observations. We also present a "simulation atlas" that shows halos produced by crystals of different shapes and for different light-source elevations and distances between the observer and the light source. The simulation method also admits a three-dimensional visualization of the phenomena.

OCIS codes: 010.1290, 010.2940, 010.3920.

1. Introduction

Atmospheric halos are normally observed in light from the Sun or the moon when the light is shining through high-level ice clouds. In geographical regions with cold winter climates, halo-producing ice crystals are also formed in layers close to the ground and even on the ground, and there halos can be observed also in connection with artificial light sources, such as street lamps. When viewed close to the source, the divergent light rays from this may greatly modify the geometry of the halos and may also reveal impressive three-dimensional shapes.

Surprisingly little research has been done on divergent-light halos. This is probably due to the lack of good photographs of the phenomena. The few articles written on the subject have treated only the most commonly seen features–light pillar, 22° halos, subsuns, and parhelia.[1–6] Whereas many halos seen in parallel light have been studied extensively with computer simulations, simulations of halos in divergent light are almost completely lacking. To our knowledge Walter Tape is the only scientist who has made some simulations of this kind.[7]

In this paper we treat some halos that appear in the divergent light from a nearby source. We will discuss these halos using both observations, some of them documented by photographs, and using a new computer simulation method.

2. Transformation of Some Halo Features by Divergent Light

The 22° and 46° halos are formed by a minimum deviation of light passing through more-or-less randomly oriented column or plate crystals, the 22° halo through 60° prisms, the 46° halo through 90° prisms. When seen in the divergent light from a nearby source these halo rings are transformed into cigarlike shapes, described by Minnaert[1] in 1928.

The parhelic circle is produced by light reflected in suitably oriented, vertical crystal surfaces. In parallel light, as from the Sun or the moon, the crystals producing this halo are located on the surface of a right circular cone with a vertical axis and with its vertex in the eye of the observer. The halo is perceived as an arc passing through the light source and parallel to the horizon.

In divergent light from a nearby source situated obliquely above the observer, the vertical crystal surfaces reflecting light toward the observer are located on a distorted "double cone" with one vertex in the light source and the other one in the eye (Fig. 1).

It can be shown that the equation of this surface is

$$z = \frac{h(x^2 + y^2)^{1/2}}{(x^2 + y^2)^{1/2} + [(x - a)^2 + y^2]^{1/2}},$$

where the observer is located in (0, 0, 0) and the source is located in (a, 0, h).

The distortion depends on the elevation of the light

L. Gislén (larsg@thep.lu.se) is with the Department of Theoretical Physics and J. O. Mattsson is with the Department of Physical Geography and Ecosystems Dynamics, Lund University, Sweden.

Received 13 January 2003; revised manuscript received 28 April 2003.

0003-6935/03/214269-11$15.00/0

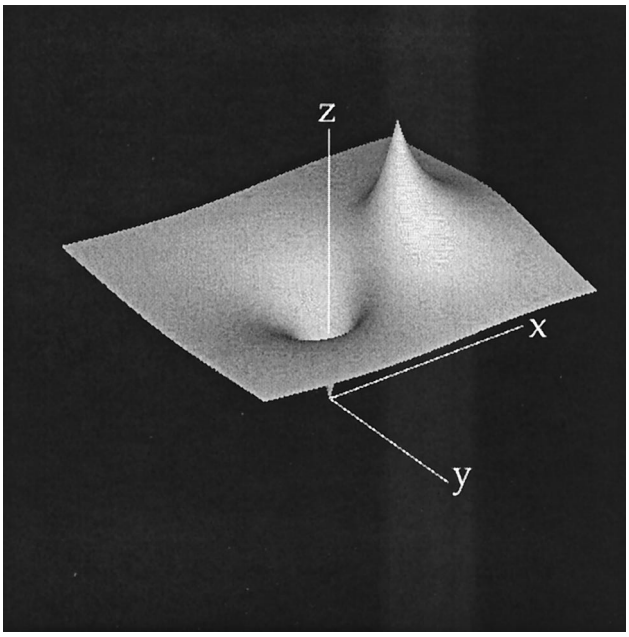

Fig. 1. Locations of ice crystals forming the parhelic circle in light from a nearby pointlike source situated obliquely above the observer. The crystals are located on a distorted "double cone" with one vertex in the light source and the other one in the eye. Source elevation 45°.

source. The surface continues asymptotically as a horizontal plane at infinity. In a divergent light halo, the parhelic arc is relatively broad with a diffuse outer border. It is more distinct close to the light source with a particularly strong light gradient towards the central dark area. (See also observation and simulations presented in Figs. 3 and 6.)

With a more distant light source the halo-producing role of those crystals that form the part of the cone with its apex in the eye of the observer will dominate, and the surface gradually will be reduced to a right circular cone in the limiting case of parallel light.

Parhelia are caused by a minimum deviation in crystals with vertical refracting edges. The crystals are plates with essentially horizontal basal faces. Straightforward geometrical considerations tell us that the crystals causing the parhelia in divergent light would be located in points forming two curved lines from the light source to the eye of the observer. As seen by the observer these points are situated on the parhelic circle on the arc segment between the ordinary parallel light parhelia and the light source. The observer will therefore perceive the parhelia as extended toward the light source.

Superparhelia are also due to refractions in oriented plate crystals, but with an additional reflection in the upper basal face of the crystal. Superparhelia are not seen in parallel light unless the light source is below the observer's horizon, which is normally not the case. However, they may be seen in divergent light when the source is obliquely above the observer. As with the parhelia, the crystals causing the superparhelia are located along two curved lines from the light source to the eye of the observer. However, as seen by the observer, the crystals form two bright curves pointing obliquely upwards and outwards from the source.

Light pillars above the sun or the moon are caused by reflection in the lower basal face of oriented, slightly tilted plate crystals as well as by internal reflection in their upper basal face. Analogously, light pillars below the light source are caused by reflection in the upper basal face of such plate crystals or by internal reflection in their lower basal face. Pillars can also be caused by reflections in the side faces of columnar crystals with the crystal axis horizontal. If the plate crystals are sufficiently oriented, the lower pillar becomes a more or less elongated spot below the horizon, the subsun.

The light pillars in divergent light are produced by the same mechanism.[8] However, the pillars may in this case also be produced by crystals without a tilt. The crystals producing the pillars are then located at points at different levels in a vertical plane through the eye of the observer and the light source and at different horizontal distances from the source. The presence of the ground surface often reduces the lower pillar to a subsun.[2]

The circumzenithal arc and the circumhorizontal arc are both produced by refraction in more-or-less oriented plate crystals. The circumzenithal arc is formed by rays entering the basal face and exiting from a side face. For the circumhorizontal arc the ray enters the side face and exits through the basal face.

In parallel light the circumzenithal arc is centered on the zenith when the Sun or the moon are at an altitude of less than 32°. The circumhorizontal arc is parallel to the horizon, below the altitude of the light source, and is seen only when the altitude of the light source is larger than 58°. The circumzenithal and circumhorizontal arcs may in divergent light also be seen for other elevations of the light source. The

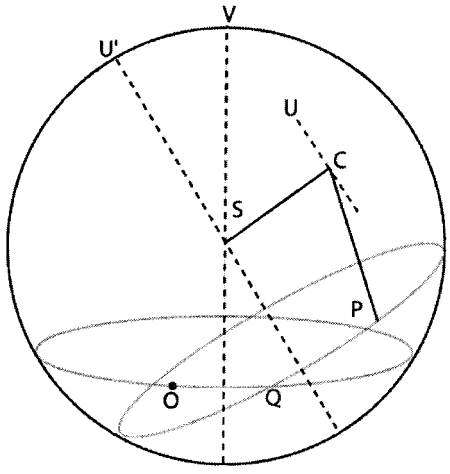

Fig. 2. Rotations on the sphere that move the hitpoint of the scattered ray into the eye of the observer.

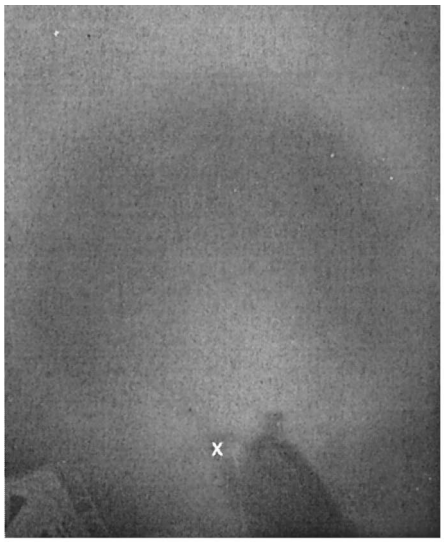

(a)

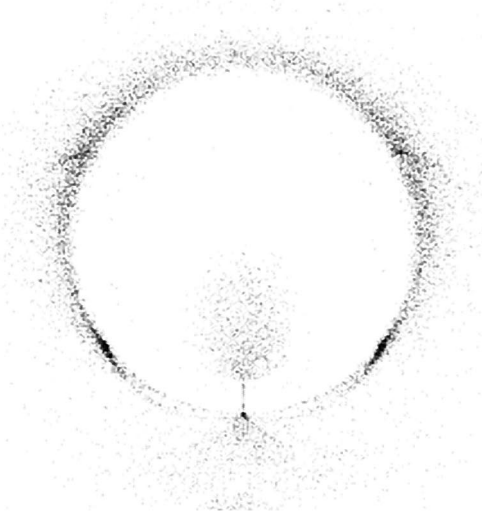

(b)

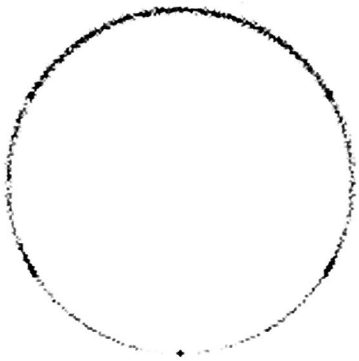

(c)

Fig. 3. (a) Parhelic circle in the light of a nearby street-lamp. The lamp elevation is 53°. Observation and photograph by Marko Riikonen. The position of the light source is marked by a small cross on the photo. (b) Simulation of the halo observation. (c) Parallel light simulation for comparison.

(a)

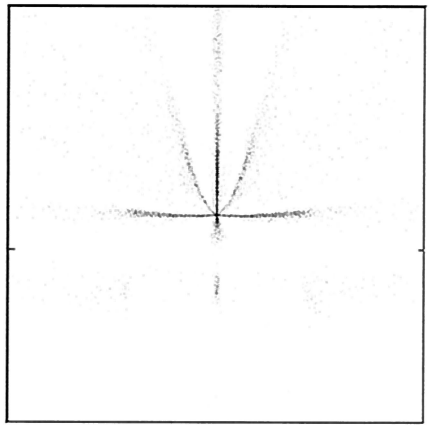

(b)

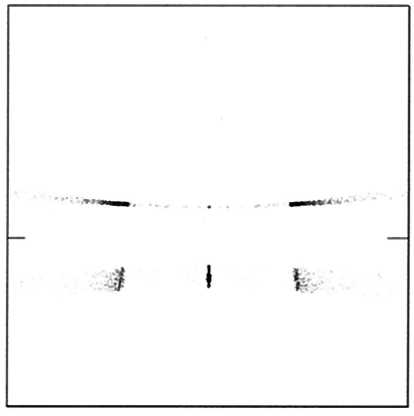

(c)

Fig. 4. Divergent-light display, including parhelia, superparhelia, and a light pillar. Observation by Marko Riikonen and Leena Virta. Photograph by Marko Riikonen. (b) Simulation of the display; (c) parallel light simulation for comparison.

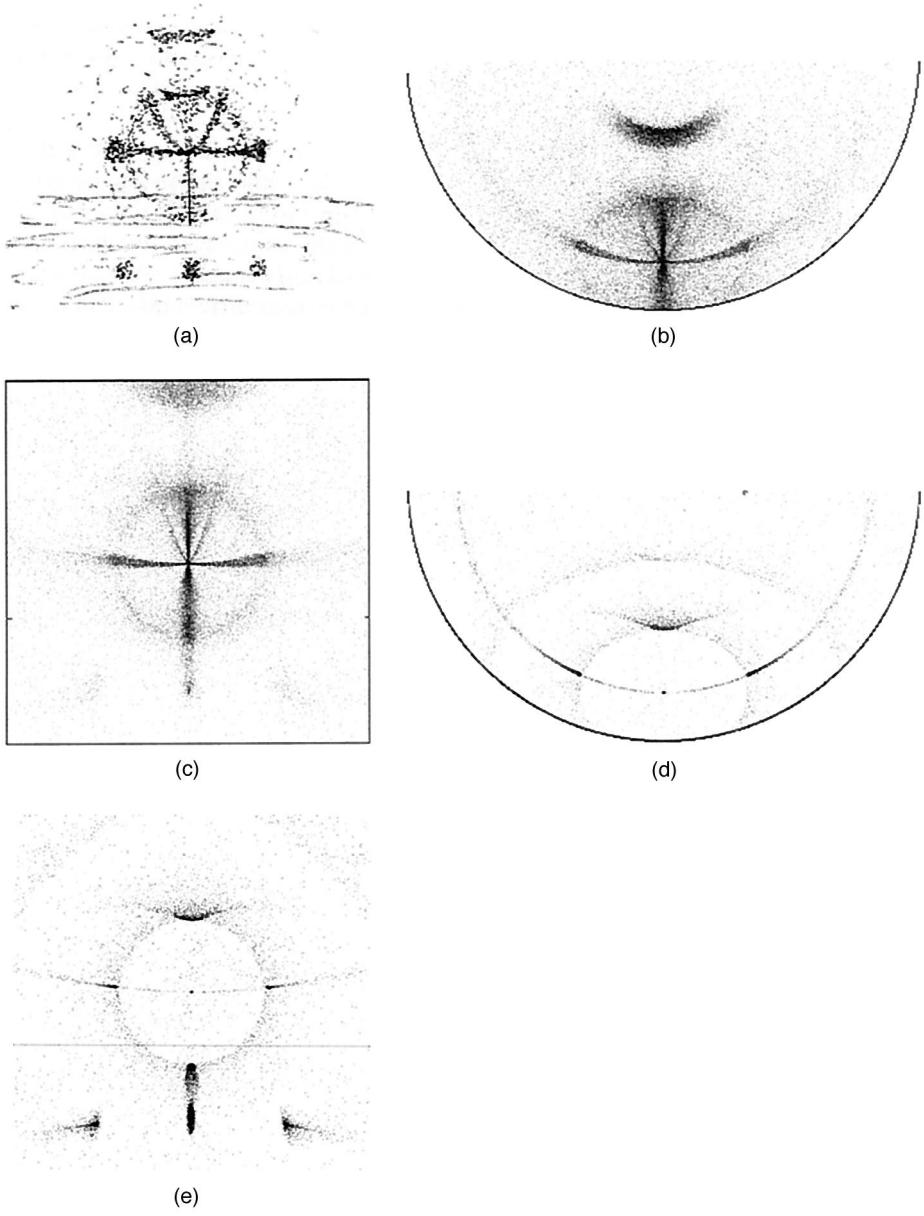

Fig. 5. (a) complex halo observed by Teemu Öhman, who also made the sketch. (b) Fisheye simulation of the display. (c) Details of the simulated halo around the sun. (d) and (e) Parallel light simulations for comparison.

forms of such halos will also be different from the forms in parallel light.

3. Simulation Procedure for Divergent-Light Halos

The method of handling the simulation of a divergent-light halo will be described in detail elsewhere,[9] and we will here give only an outline. We refer to Fig. 2 for our description. The source S is the centre of a sphere. The observer O is located on the surface of the sphere.

We generate a ray in a random direction that starts from the source S and hits a crystal at C. We trace the ray through the crystal from which the ray emerges as a scattered ray CP, where P is located on the surface of the sphere. In most cases P will not coincide with the observer's position at O. However, it is sometimes possible, by two symmetry rotations, one around an axis parallel to the symmetry axis of the crystal and one around the vertical, to make P coincide with O. In the case shown in Fig. 2 we can first make a rotation around the axis U′, parallel to the symmetry axis U of the crystal, to move the hit-point from P to Q, and then a second rotation around the vertical axis V. This second rotation will take the point Q to O. The observer will then register a bright point in the sky in the reverse direction of the direction CP thus rotated. The computer program checks all points along SC and chooses randomly

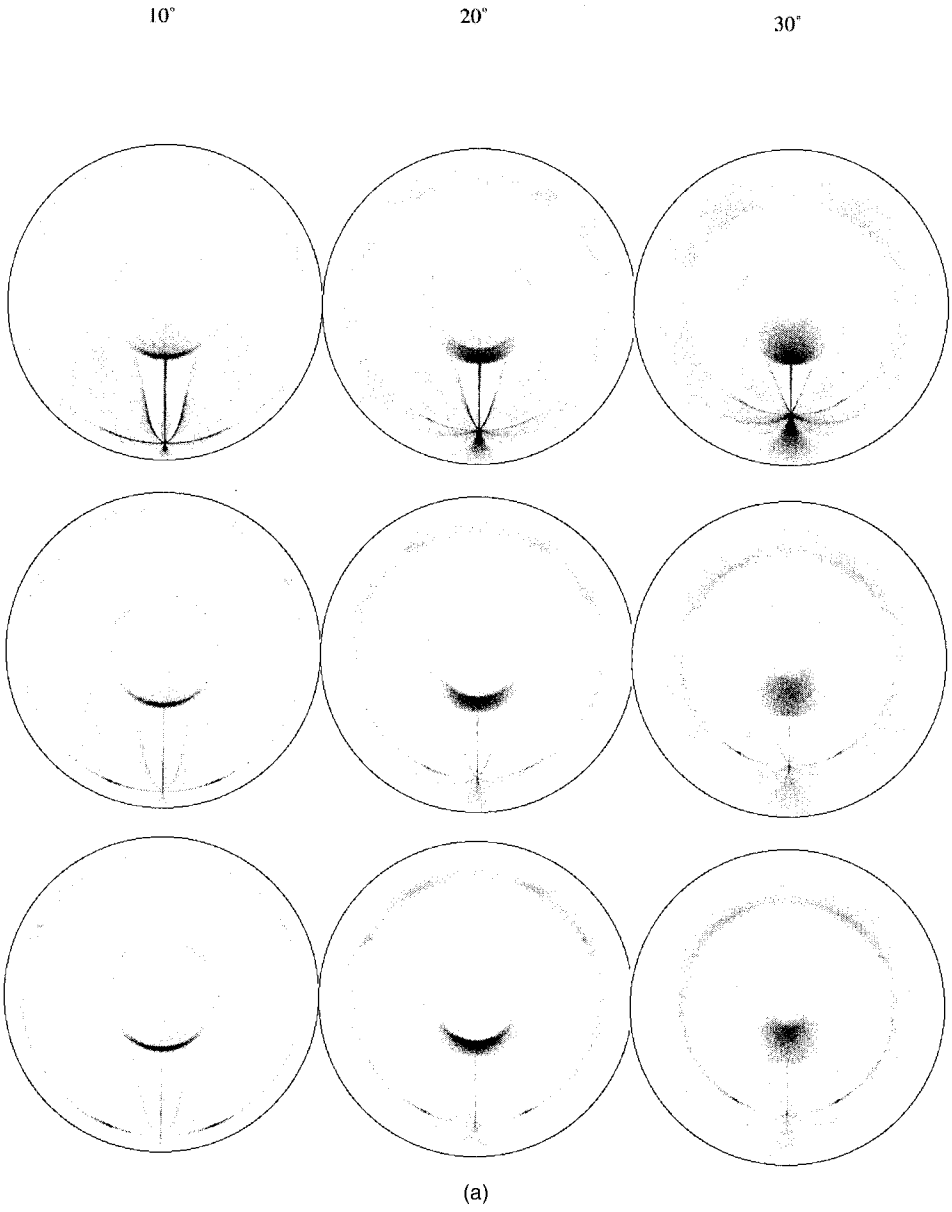

Fig. 6. Simulation of halos by plate crystals (c/a ratio 0.3, tilt 0.5°) for different source elevations and distance parameters. The top row represents a light source very nearby (distance parameter $p = 0.01$), the middle row represents a somewhat more distant source ($p = 0.05$), and the bottom row represents a distant source ($p = 0.1$).

from the ones (if any) that result in a ray that can be made to hit the observer.

The angle that U makes with V is the tilt angle of the crystal. If the tilt angle is 90°, the two rotation axes are perpendicular and we will be able to reach, by the rotations, any point on the sphere; we will always succeed in bringing the scattered ray into the eye of the observer. On the other hand, if the tilt angle is zero the two axes will be parallel, and we will reach only a very limited number of points on the sphere. For instance if, in the situation shown in the figure above, the tilt axis had been vertical, we would have been able to reach only points on the horizontal parallel circle through P. Thus for small tilt angles very few of the scattered rays can be brought to the eye. This will influence the intensity of the halo in certain regions of the sky, especially for crystals with a small tilt from the vertical. The computer algorithm will have problems to define the rotations when the tilt is exactly zero. We therefore set all tilts less than 0.01° as equal to 0.01°.

There is a further problem with divergent-light halos that must be handled. For a parallel light halo, the active crystals are located anywhere along the direction of the scattered ray that hits the eye. The intensity of the halo in that direction will be the sum of the contributions from many crystals along that direction. For a divergent light halo this is not the case. Because of the geometrical constraints, crystals have to occupy specific locations in space. The

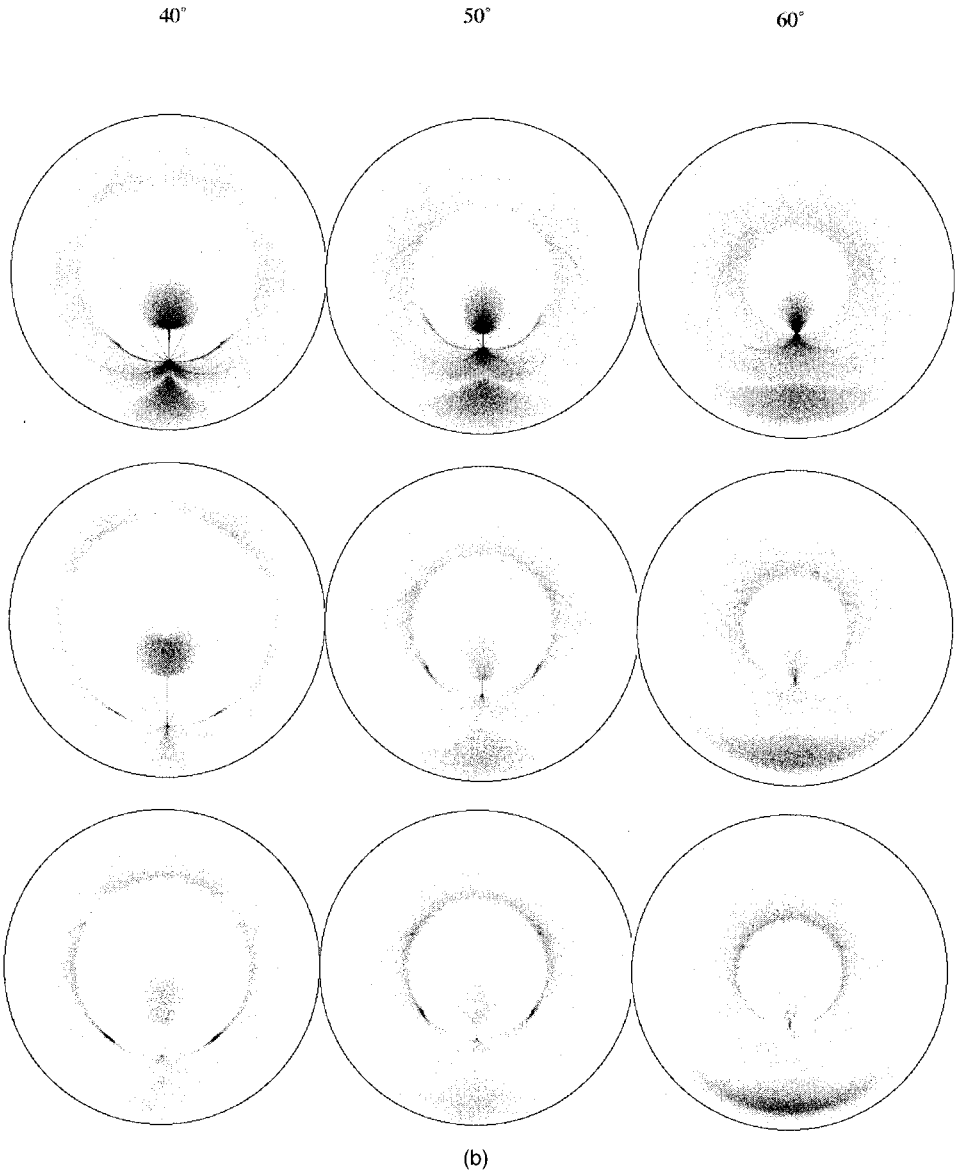

(b)

Fig. 6. Continued.

lightwaves of the ray scattered by a crystal will be confined in width by the "size" of the crystal. This means that we have to take into account diffraction. If the crystal is located close to the eye, the diffraction spot will be small and all the light of the ray will enter the pupil of the eye. As we increase the distance to the crystal the diffraction spot will grow in size, but as long as it fits within the aperture of the pupil most of the light will still enter the eye. Thus, up to a certain distance, the intensity of the ray will be perceived as more or less constant. At larger distances the diffraction spot will be larger than the pupil, and only a fraction of the light will enter the eye. At larger distances we then expect the intensity to fall off as the inverse square of the distance to the crystal. We can handle this mathematically by integrating the intensity of the diffraction spot over the area of the pupil for different distances to the crystal. It turns out that we can describe the resulting decrease in intensity by weighting the probability of each generated scattering event being plotted by the very simple factor

$$I \propto \frac{a^2}{a^2 + t^2}, \qquad \text{where } a = \frac{d_p d_C}{\lambda D},$$

where t is the parametric distance from observer to crystal, i.e. the distance observer–crystal measured in units of the distance observer–source; d_P is the diameter of the pupil; d_C is the size of the crystal, i.e. some average diameter; λ is the wavelength of the light, and D is the distance from observer to source. Assuming a standard pupil size (6 mm) and a standard wavelength (600 nm), we see that the intensity depends via a on the distance parameter $p = D/d_C$. We use units such that D is measured in meters and

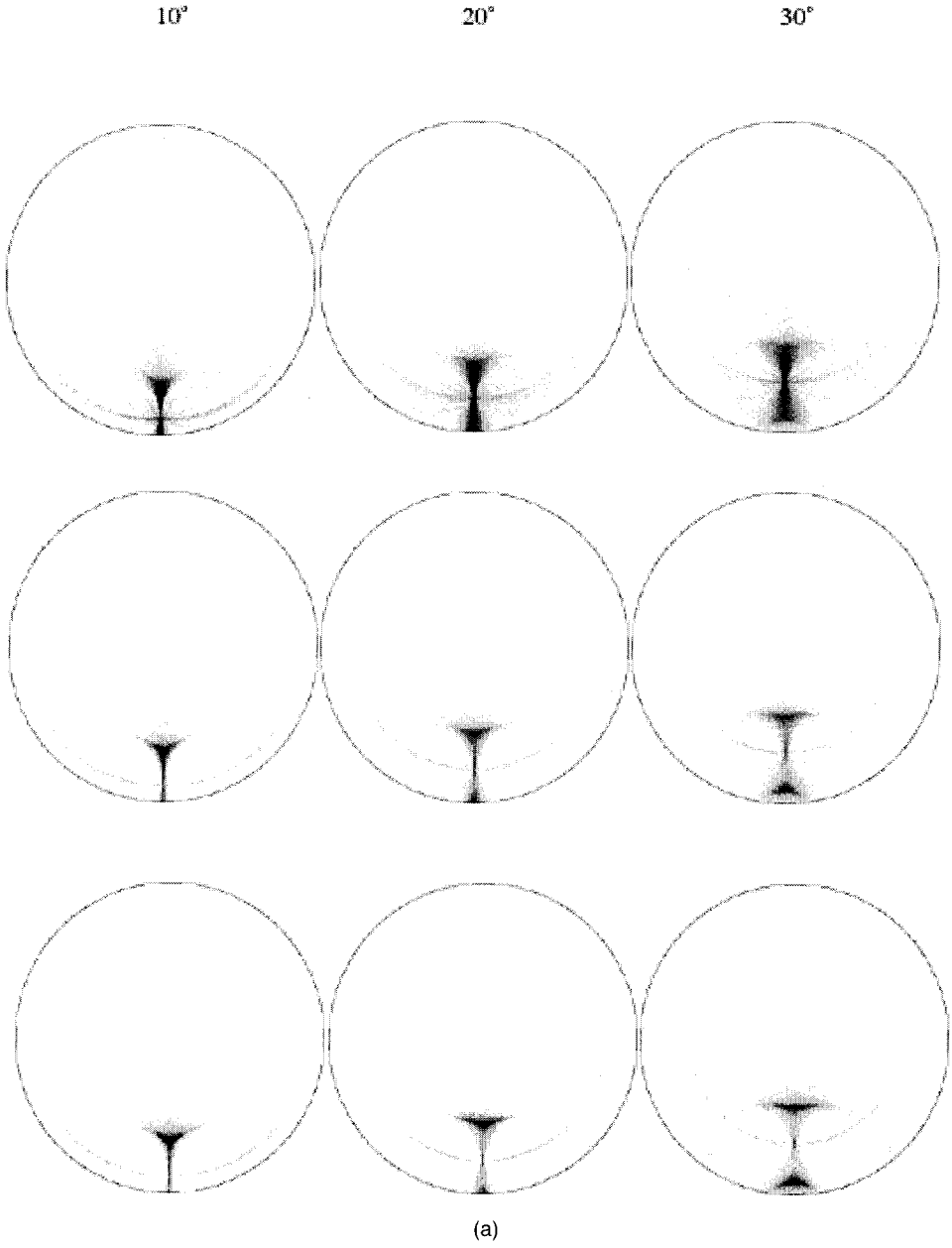

Fig. 7. Simulation of halos by columnar crystals (c/a ratio 2.0, tilt from the horizontal 0.5°) for different source elevations and distance parameters. The distance parameters are the same as in Fig. 6.

d_C in micrometers. Typical crystals in a halo have sizes of the order of 100 μm. Then $p = 1$ corresponds to a distant halo ($D = 100$ m) and $p = 0.01$, to a very nearby halo ($D = 1$ m). The appearance of a divergent-light halo will depend on the ratio of the distance of the observer from the source and the size of the crystals. This means that in a complex halo display with ice crystals of several sizes we can have different distance parameters for different features. An example of this is given in Fig. 5. One further interesting consequence of the intensity formula is that the appearance of the halo will depend on the aperture of the eye. If the halo is photographed with a camera that has a lens aperture that is larger than the pupil of the eye by a factor of k, the effective distance parameter will change by a factor of $1/k$, and the halo will show more nearby features in the photo. This is a prediction that can be tested in the field.

The computer program also gives the precise location in space of the scattering crystals. Using this information we can generate stereo pictures of a halo. A PASCAL version of the program unit used to handle the rotations can be found at http://www.thep.lu.se/~larsg/, where simulated stereo pictures of some divergent-light halos can also be found.

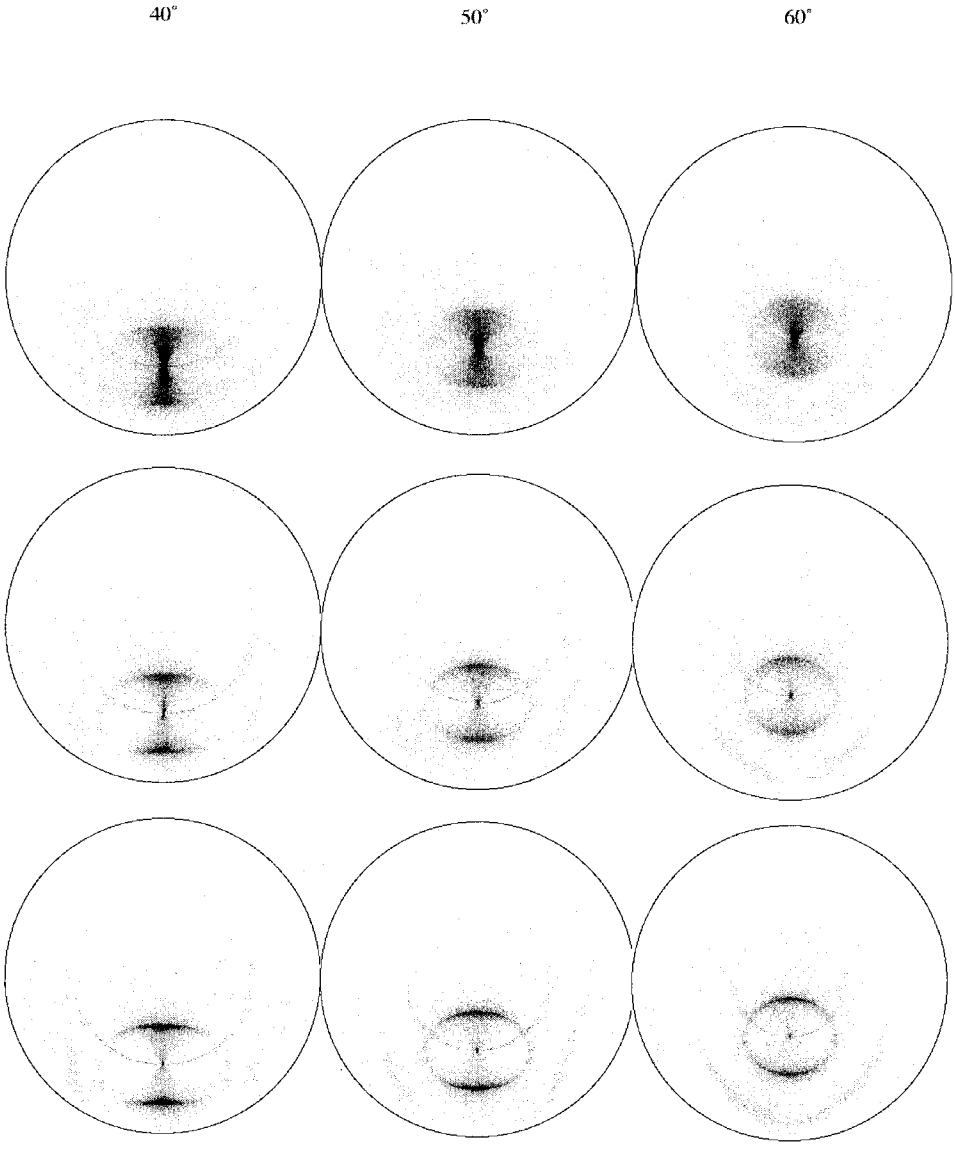

(b)

Fig. 7. Continued.

4. Observations and Simulations of Some Halos in Divergent Light

A complete parhelic circle in the light of a street lamp was observed and photographed by Marko Riikonen on 17 March 2001 in Oulu, Finland [Fig. 3(a)].

The observation was made at a temperature of −18 °C, and the ice crystals were generated by a steam plume from a paper factory a few kilometers away. The light source was situated quite near the observer (photographer), obliquely above him at an elevation of approximately 53° [Fig. 3(a)]. The display lasted for at least 1 h. According to the observer it was an amazing sight to look into the glowing, three-dimensional "vortex" of the parhelic circle above his head.

As seen in the figure, a fairly broad parhelic circle surrounds a dark area. The inner border of the circle is more distinct than the outer one.

Figure 3(b) shows a simulation of this observation with plate crystals with c/a ratio equal to 0.3, tilt 0.5°, and distance parameter 0.05. The simulation also includes parhelia not clearly seen in the photograph. For comparison we also show a parallel light halo simulation in Fig. 3(c).

A nice divergent-light halo display was observed by Marko Riikonen and Leena Virta on the night of 12–13 December 1999 in Kaamanen in northern Finland. The display, which was also photographed by Marko Riikonen [Fig. 4(a)], included parhelia, superparhelia, and a light pillar.

The photograph was taken about 50 m from the light source. The elevation of the lamp was estimated to be about 10°. At this distance the halo did not have any strong three-dimensional features. Parhelia started to curve inwards toward the observer only when the observer walked approximately 20 m closer to the

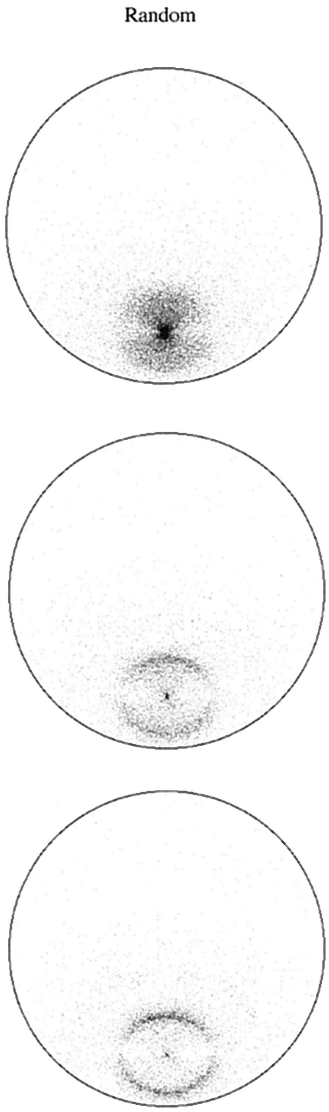

Fig. 8. Simulations of halos by randomly oriented crystals with c/a = 1.0 and for different distance parameters (0.01; 0.05; 0.1). Source elevation is 30°.

lamp, when the circumzenithal arc also appeared. No signs of a parhelic circle were seen. The display vanished slowly after lasting for several hours. The air temperature was −20 °C, and the wind was light. The white pillar streching downwards from the lamp is not part of the halo, but of the lamp pole. In Fig. 4(b) we simulate this display. We used plate crystals with a tilt of 2° and a small distance parameter of 0.02. We also applied a ground cutoff to restrict the features below the horizon. Figure 4(c) shows a parallel light simulation of the same halo.

In Figs. 5(b) and 5(c) we have tried to simulate a complex halo [Fig. 5(a)] observed by Teemu Öhman in Oulu on 15–16 January 2000.[7] This display has an interesting mixture of both divergent and parallel light halo features. There are prominent parhelia streching towards the sun, two arc-shaped superparhelia rising obliquely from the source, a circumzenithal arc, an upper tangent arc (plume), and a faint lower tangent arc plume. All these features are typical of divergent light halos. Further we see an ordinary annular halo, a typical parallel light feature generated by a more or less randomly oriented crystals. With a nearby light source the annular halo would have been disklike (see Fig. 8, top). We can simulate the divergent light features using comparatively large oriented crystals giving a small distance parameter and smaller randomly oriented crystals having a larger distance parameter for the same observer–source distance. For the simulation we assumed a source elevation of 17.5° and used plate crystals (c/a = 0.3) and columnar crystals (c/a = 2) with a tilt of 2° and a distance parameter of 0.02 and randomly oriented crystals with a distance parameter of 0.1. The visual observation also shows two subparhelia and a subsun, which are not shown in the fisheye simulation. Figures 5(d) and 5(e) show parallel light simulations for comparison.

5. Simulation Atlas

Figures 6–9 show fisheye simulations for different crystal types and different light source elevations. The zenith angle is proportional to the distance from the center of the circular plot, being 90° at the perimeter of the circle. The maximum distance parameter used was $p = 0.1$. The reason for this is twofold. With this distance parameter the halo has more or less lost all of the divergent-light features, as can easily be seen by comparing with published ordinary halo simulations.[10,11] Secondly, the simulation algorithm is very inefficient for large distance parameter values when only crystals relatively close to the eye will contribute to the intensity, and the simulations become very time-consuming.

We first show a set of simulations for plate crystals (c/a ratio 0.3, tilt 0.5°) and for different source elevations ($h = 10°, 20° \ldots 60°$); Figs. 6(a) and 6(b). The top row shows simulations for a distance factor of $p = 0.01$ (very close halos), the middle row has $p = 0.05$, and the bottom row has $p = 0.1$. Assuming a size of the ice crystal of 100 μm, a standard eye pupil size of 6 mm and a light wavelength of 600 nm, this corresponds to actual distances of 1, 5, and 10 m, respectively. Larger crystal sizes would scale these distances in proportion.

Typical for plate crystals at low elevations of the source are the strong superparhelia stretching out obliquely and upwards from the source. We also have a strong vertical pillar, and parhelia are reaching horizontally inwards to the source. As the elevation of the source increases, the superparhelia become shorter and have disappeared at an elevation of 60°. An interesting feature that can be seen especially for higher elevations are the 120° parhelia, the thin and faint arcs that start at the source and end in the location of the ordinary parallel-light 120° parhelia. However, these parhelia disappear for crystals at larger tilts and probably would be hard to see in the field. The circumzenithal arc is fairly sharp at lower elevation and is transformed into a

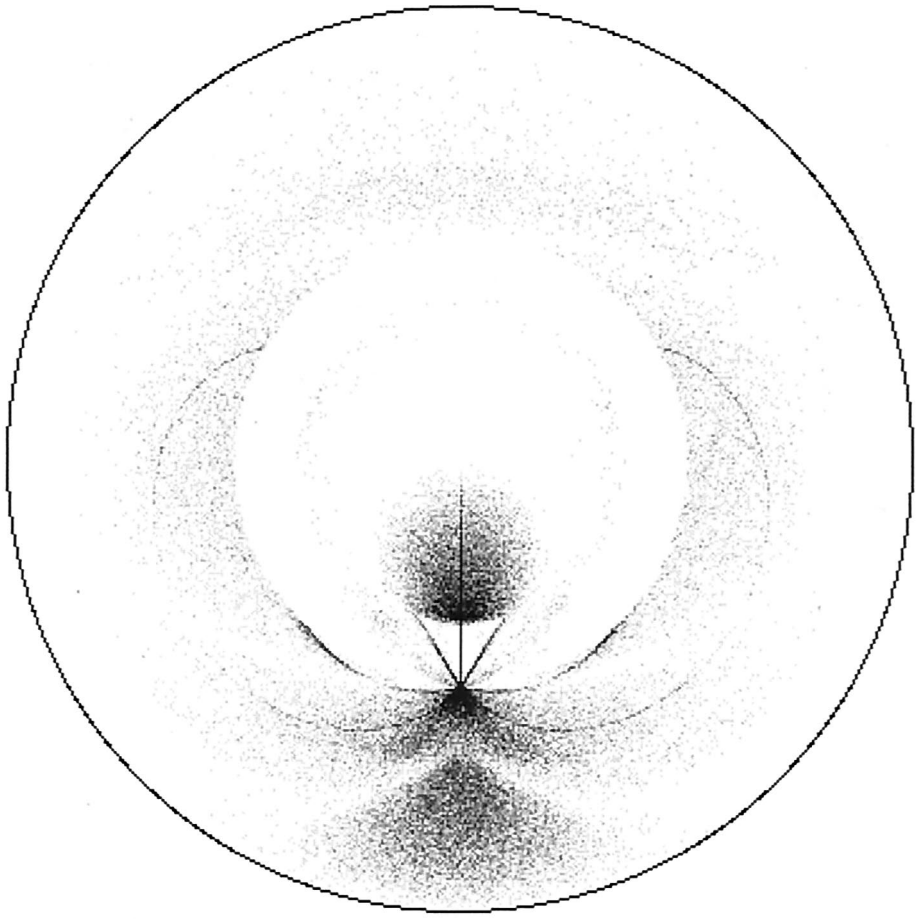

Fig. 9. Simulation of a halo by plate crystals (c/a = 0.3) with very small tilts to show the 120° parhelia. The source elevation is 45°.

patch for higher elevations, reaching the light source for the highest source elevation in the atlas below. The circumhorizontal arc shows up already at small elevations as a plume downward from the source.

As we move out from the source, the features specific for the divergent-light halo fade away, and the halo looks more and more like a parallel-light halo.

For columns, Figs. 7(a) and 7(b), c/a = 2.0, tilt from the horizontal 0.5°, there are fewer features. The intense plume stretching downwards towards the source is the upper tangent arc. The corresponding plume below the source is the lower tangent arc. As the elevation increases the tangent arcs flatten out, and for elevation 60° they have formed a more or less circumscribing halo. Again, as we move away from the source, the halo is gradually transformed into the ordinary parallel-light circumscribed halo.

Figure 8 shows simulations for randomly oriented crystals (c/a = 1.0) at different distances from the source. Near the source we get a circular patch of light generated by crystals that are located within a cigar-shaped region between the observer and the source. Away from the source the patch is transformed into the ordinary 22° halo. There is a horizontal region with a lower intensity in this halo that will almost disappear as the elevation of the source increases. This is, as explained earlier, due to the fact that this part of the halo is generated by crystals with predominantly vertical symmetry axes, i.e. with small tilts. The probability that scattered rays from such crystals will hit the eye is very small.

6. Final Remarks

It must be remembered that the simulation model we use is very idealized. It assumes perfect, textbook, hexagonal crystals. It also assumes that the light source is pointlike and that the emitted light rays are completely unobstructed in all directions, which is rarely the case. Many street lights have reflectors that block the light in some directions, which can modify the display substantially. Another assumption is that the crystal distribution is homogeneous and extends unlimited upward and downward in space.

The simulations give all possible halos. One example is the faint 120° parhelia commented on above, which have probably never been seen so far. (A simulation of this phenomenon can be seen in Fig. 9.) One problem is also that we have one extra parameter to play with, the distance parameter, in a divergent-light halo. However, we believe that knowing what to look for makes it easier to find a feature. The simulation method, within the limits pointed out above, seems to give results that agree

reasonably well with observations. More field observations of these halos are strongly encouraged and if possible documented by photographs. In this context it is important also to document the aperture size of the camera, as this directly influences the appearance of the halo. Information on the crystal sizes is important. It is also vital to have observations done very near to the source and to document changes in the halo display as the halo is approached. It should also be noted if the light from the source is obstructed in any direction.

We are greatly indebted to Marko Riikonen, Ursa Astronomical Association, Helsinki, Finland for allowing us to use his photographs of halo phenomena in divergent light and for critical remarks and stimulating discussions.

References and Note

1. M. Minnaert, "Een halo in de onmiddellijke nabijheid van het oog," Hemel en Dampkring **26,** 51–54 (1928).
2. J. O. Mattsson, "Sub-sun and light pillars of street lamps," Weather **28,** 66–68 (1973).
3. J. O. Mattsson, "Experiments on horizontal haloes in divergent light," Weather **29,** 148–150 (1974).
4. C. Floor, "Rainbows and haloes in lighthouse beams," Weather **35,** 203–208 (1980).
5. J. O. Mattsson, "Concerning haloes, rainbows and dewbows in divergent light," Weather **53,** 176–181 (1998).
6. J. O. Mattsson, L. Bärring, and E. Almqvist, "Experimenting with Minnaert's Cigar," Appl. Opt. **39,** 3604–3611 (2000).
7. Brief reports on the parhelic circle in divergent light are given in the Finnish journal Ursa Minor, published in Finnish, with some figure captions in English, by Tähtitieteellinen yhdistys Ursa in Helsinki. The pages and issues in question are 11, 1/2000 (a simulation by Walter Tape of a surface similar to the one in Fig. 1) and 13–14, 3/2001 (some observations).
8. A. J. Mallmann, J. L. Hock, and R. G. Greenler, "Comparison of sun pillars with light pillars from nearby light sources," Appl. Opt. **37,** 1441–1449 (1998).
9. L. Gislén, "Procedure for simulating divergent-light halos," Appl. Opt., submitted for publication.
10. W. Tape, *Atmospheric Halos* (American Geophysical Union, Washington, D.C., 1994).
11. R. Greenler, *Rainbows, Halos, and Glories* (Printstar Books, Milwaukee, Wisc., 1999).